Site-Specific Mutations in the Myosin Binding Sites of Actin Affect Structural Transitions That Control Myosin Binding[†]

Ewa Prochniewicz* and David D. Thomas

Department of Biochemistry, Molecular Biology, and Biophysics, University of Minnesota, Minneapolis, Minnesota 55455

Received May 2, 2001; Revised Manuscript Received July 23, 2001

ABSTRACT: We have examined the effects of actin mutations on myosin binding, detected by cosedimentation, and actin structural dynamics, detected by spectroscopic probes. Specific mutations were chosen that have been shown to affect the functional interactions of actin and myosin, two mutations (4Ac and E99A/E100A) in the proposed region of weak binding to myosin and one mutation (I341A) in the proposed region of strong binding. In the absence of nucleotide and salt, S1 bound to both wild-type and mutant actins with high affinity ($K_d < \mu$M), but either ADP or increased ionic strength decreased this affinity. This decrease was more pronounced for actins with mutations that inhibit functional interaction with myosin (E99A/E100A and I341A) than for a mutation that enhances the interaction (4Ac). The mutations E99A/E100A and I341A affected the microsecond time scale dynamics of actin in the absence of myosin, but the 4Ac mutation did not have any effect. The binding of myosin eliminated these effects of mutations on structural dynamics; i.e., the spectroscopic signals from mutant actins bound to S1 were the same as those from wild-type actin. These results indicate that mutations in the myosin binding sites affect structural transitions within actin that control strong myosin binding, without affecting the structural dynamics of the strongly bound actomyosin complex.

Force generation in muscle results from cyclic interactions between actin and myosin heads in the presence of ATP. A major step toward understanding the mechanism of these interactions was the solution of X-ray crystal structures for the actin monomer (*1*) and the myosin head (S1)[1] (*2*), and models of the actin−myosin interface were created by fitting these high-resolution structures into the low-resolution electron density maps of acto-S1 obtained from cryoelectron microscopy (*3, 4*).

These structural models gained support from functional effects of mutations in the proposed myosin-binding regions of actin from yeast. The mutation E99A/E100A, localized in the N-terminus, which is proposed as the region of weak interactions, was shown to inhibit functional interactions with myosin (activation of myosin ATPase and sliding in the in vitro motility assay); this inhibition was attributed to the altered electrostatic charge of actin (*5−7*). The I341A mutation, localized in the hydrophobic helix 338−348, which is proposed to contribute to strong binding, also has significant inhibitory effects (*8*). On the other hand, the change of the yeast sequence M-D-*S*-E into the muscle-like sequence M-D-*E-D*-E by the 4Ac mutation increased the

catalytic efficiency of actin, supporting the model-indicated role of the sequence at the extreme N-terminus of actin in the function of actomyosin (*6*). The functional effects of mutations in *Dictyostelium* and *Drosophila* actins were also explained in terms of changes in the regions of interaction with myosin, as proposed by the structural models (*9, 10*).

However, the specific sequences in the proposed regions of interaction with myosin, indicated in the structure of the actin monomer, are not sufficient for effective functional interactions, as indicated by the requirement of actin polymerization for activation of myosin ATPase. Observations in the electron and optical microscopes have shown that the actin filament is flexible (*11−13*) and inspired studies that demonstrated the importance of actin's dynamics in the mechanism of functional interactions with myosin. Actin's flexibility is affected by binding of myosin in rigor (no nucleotide) as well as during active interactions (*12, 14*), and these changes are probably related to myosin-induced changes in the rates and amplitudes of internal motions in actin, detected in numerous spectroscopic studies (*15−17*). The complex relationship between actin's structural dynamics and the function of actomyosin has been supported by the effects of chemical cross-linking, which inhibited sliding movement in the in vitro motility assay and significantly decreased the amplitude of the rotational motions in the actin filament without inhibiting activation of myosin ATPase (*18, 19*).

The three above-mentioned mutants of yeast actin (4Ac, E99A/E100A, and I341A) provide a useful model to study the molecular basis of mutation-induced changes in functional interactions of actin. Previous functional and biochemical studies led to the proposal that the molecular

[1] Abbreviations: ErIA, erythrosin iodoacetamide; IAEDANS, 5-((((2-iodoacetyl)amino)ethyl)amino)naphthalene-1-sulfonic acid; S1, myosin subfragment 1; TPA, transient phosphorescence anisotropy; PMSF, phenylmethanesulfonyl fluoride; TLCK, *N*-*p*-tosyl-L-lysine chloromethyl ketone; TPCK, *N*-tosyl-L-phenylalanine chloromethyl ketone; BAAE, *N*α-benzoyl-L-arginine ethyl.

mechanism of these mutations involves effects on structural transitions in the actomyosin ATPase cycle (*5, 6, 8, 20*). In the present study we use optical spectroscopy (transient phosphorescence anisotropy, TPA, and fluorescence) to test this possibility by measuring the effects of mutations on the structural dynamics of yeast actin alone and in complexes with myosin heads isolated from rabbit muscle. The experiments on actomyosin complexes are limited to the strongly bound states in the absence of nucleotide (rigor) and in the presence of ADP. The effect of ADP was of particular interest, since studies on the skeletal actin−myosin system suggest that actin−S1−ADP complexes play an important role in the cross-bridge cycle (*21*). By measuring quantitatively the binding of S1 to actin under the conditions of the spectroscopic measurements, we were able to determine independently the effects of the mutations on actin binding, on the structural dynamics of isolated actin filaments, and on the structural dynamics of the bound ternary complex, actin−myosin−ADP.

MATERIALS AND METHODS

Preparation of Proteins from Muscle. Skeletal muscle actin was prepared as described previously (*15*) by extracting acetone powder of rabbit skeletal muscle with cold water, polymerizing with 30 mM KCl for 1 h at room temperature, and centrifuging for 1 h at 200000*g*. The pellet was suspended in G−Mg buffer (5 mM Tris, pH 7.5, 0.5 mM ATP, 0.2 mM MgCl$_2$). Myosin subfragment 1 (S1) was obtained by α-chymotryptic digestion of myosin from rabbit skeletal muscle (*22*).

Preparation of Yeast Actin. Yeast strains were generous gifts from P. Rubenstein (4Ac) and E. Reisler (E99A/E100A, I341A). Wild-type yeast actin and mutant actins were purified using DNase affinity column chromatography, as described previously (*23*). One hundred ten grams of a wild-type yeast cake or 120 g (wet weight) of mutant yeast cell pellets was added to an equal volume of Y−G buffer (10 mM Tris, pH 7.5, 0.2 mM CaCl$_2$, 0.2 mM ATP) with protease inhibitors (20 μM PMSF and 10 μg/mL each of aprotinin, leupeptin, antipain, pepstatin, chymostatin, TLCK, TPCK, and BAAE). An equal volume of acid-washed glass beads was added, and cells were lysed at 4 °C in a bead beater by 12 cycles of beating (20 s beating followed by 3 min break). Cell debris was pelleted by 1 h centrifugation at 200000*g*, and the supernatant containing actin was applied on the Affi-Gel DNase column equilibrated with Y−G buffer with protease inhibitors. The column was sequentially washed with Y−G buffer with protease inhibitors, with Y−G buffer with 0.4 M NaCl, and with Y−G buffer. The outlet of the DNase column was then connected to a 1 mL Whatman DE-52 column equilibrated with Y−G buffer, and actin was eluted directly onto the DE-52 column with 50% formamide in Y−G buffer. After exhaustive washing with Y−G buffer, yeast actin was eluted from the DE-52 column with 0.3 M KCl in Y−G buffer, dialyzed overnight against Y−G buffer, polymerized with 2 mM MgCl$_2$, and ultracentrifuged for 1 h at 200000*g*, and pellets were suspended in G−Mg buffer, the same as used during preparation of skeletal muscle actin.

Labeling with Optical Probes. Wild-type and mutant yeast actins were labeled with the phosphorescent dye ErIA or the fluorescent dye IAEDANS. The main advantage of ErIA is

a high ratio of phosphorescence to fluorescence, which, in combination with the high sensitivity of our TPA instrument, allows us to measure signals at submicromolar concentrations (*16*). IAEDANS is an environmentally sensitive probe that reacts specifically with Cys 374 (*24, 25*). Actin (24 μM) was polymerized with 2 mM MgCl$_2$ and 20 mM Tris, pH 7.5, and the dye, freshly dissolved in DMF, was added at a concentration of 120 μM (ErIA) or 240 μM (IAEDANS) to actin. After 1.5 h incubation at 25 °C, the reaction was stopped by addition of 5 mM DTT, actin was ultracentrifuged 1 h at 200000*g*, pellets were suspended in Mg−G buffer and clarified by 10 min centrifugation at 300000*g*, and actin was polymerized with 2 mM MgCl$_2$. After ultracentrifugation 1 h at 200000*g*, pellets were suspended in Mg−F buffer (1 mM MgCl$_2$ and 10 mM Tris, pH 7.5, containing additionally 0.2 mM ATP), and the labeled F-actin was immediately stabilized by addition of a 1.5 molar excess of phalloidin to prevent denaturation. Complete removal of free dye was confirmed by precipitating the labeled actin with acetone, centrifuging the precipitate, and measuring the absorbance (538 nm) of the supernatant; no difference with a blank containing acetone only was found. The extent of labeling, expressed as moles of dye per mole of actin, was 0.3 (ErIA) and 0.7 (IAEDANS). This low extent of labeling with ErIA was essential to prevent aggregation of the E99A/E100A mutant, and this was applied to all actins. Samples of unlabeled actin were prepared in parallel and were also stabilized with phalloidin.

Protein Concentration. The concentration of unlabeled proteins was measured by ultraviolet absorption, assuming molar extinction coefficients of 0.63 mg mL^{-1} cm^{-1} for actin at 290 nm and 0.75 mg mL^{-1} cm^{-1} for S1 at 280 nm. The concentration of labeled actin was measured using the Bradford protein assay (*26*) with unmodified actin as a standard.

Removal of Free Nucleotide from F-Actin. Commercial Dowex 1 anion-exchange resin was regenerated by sequential washes with 1 N NaOH, H$_2$O, 2 N HCl, and H$_2$O, and just before use it was equilibrated with Mg−F buffer. F-Actin stabilized with phalloidin was treated for 2 min at 4 °C with 1/3.5 volume of Dowex 1 suspended 1:1 (v/v) in the Mg−F buffer, centrifuged 2 min in a microfuge, and immediately supplemented with phalloidin (0.3 mol of phalloidin/mol of actin) to compensate for removal of free phalloidin by Dowex 1. The presence of excess phalloidin in the nucleotide-free actin was particularly important in the case of yeast F-actin, where the lower phalloidin affinity, more open nucleotide-binding cleft, and faster rate of nucleotide exchange than muscle actin could make it more susceptible to denaturation (*27*). Dowex 1 treatment resulted in removal of about 99.6% of free nucleotide, as tested with the Mg−F buffer containing 0.2 mM ATP, and the remaining nucleotide was equivalent to no more than 3% of total S1 in the acto-S1 samples.

Binding of S1 to Actin. Increasing concentrations of S1 (0.05−0.3 mg/mL) were added to 0.1 mg/mL phalloidin-stabilized unlabeled or labeled actin in the Mg−F buffer in the absence and presence of 1 mM ADP and 0.1 M KCl. Samples were ultracentrifuged for 15 min at 80000 rpm at 25 °C (Beckman TL 100 ultracentrifuge) to pellet actin-bound S1. The concentration of the unbound S1 in the supernatant was determined by measurement of the NH$_4$-Cl−CDTA ATPase activity; we have found that CDTA was

more effective than EDTA in removing free Mg^{2+} ions from the buffer. P_i was measured by the malachite green method (*28*). Control experiments showed that binding of S1 in the presence of ADP was not affected by adding hexokinase and Ap5A; i.e., the dissociating effect of ADP is not due to the presence of contaminating ATP in the samples. The dissociation constant of S1 binding to actin (K_d = [A][S1]/[A·S1]) was calculated by fitting data to the equation:

$$\frac{S1_{bound}}{A_t} = \frac{(S_t + A_t + K_d)[(S_t + A_t + K_d)^2 - 4A_tS_t]^{1/2}}{2A_t} \quad (1)$$

where $S1_{bound}/A_t$ = molar ratio of S1 bound to actin, A_t = total concentration of actin, and S_t = total concentration of S1. Data were obtained in two or three independent experiments, each of which included six to eight different S1 concentrations. Uncertainties for K_d were determined from statistical analysis of the fit using Origin 6.0.

Samples for Spectroscopic Experiments. For time-resolved phosphorescence anisotropy (TPA) experiments, phalloidin-stabilized ErIA−F-actin was diluted in Mg−F buffer to 0.06 mg/mL; to prevent photobleaching of the dye, oxygen was removed from the sample by 5 min incubation with glucose oxidase (55 μg/mL), catalase (36 μg/mL), and glucose (45 μg/mL) (*29*). For fluorescence measurements, phalloidin-stabilized IAEDANS−F-actin was diluted in the same Mg−F buffer to 0.1 mg/mL. Fluorescence experiments did not require oxygen removal, as fluorescence intensity remained at a constant level during at least 30 min illumination by excitation light.

Fluorescence and Phosphorescence. Fluorescence was measured in the ISS K2 fluorometer at 25 °C. Phosphorescence was measured at 25 °C as described previously (*15*). The actin-bound ErIA was excited with a 10 ns pulse of vertically polarized light at 540 nm, followed by detection of the time-dependent phosphorescence emission (650 nm) with a time resolution of 50 ns/channel. Phosphorescence signals were digitized with a transient recorder (dwell time 0.666 μs/channel resolution), and repeated transients were averaged by the microcomputer. The time-resolved phosphorescence anisotropy (TPA) was calculated as

$$r(t) = [I_{vv}(t) - GI_{vh}(t)]/[I_{vv}(t) + 2GI_{vh}(t)] \quad (2)$$

where $I_{vv}(t)$ and $I_{vh}(t)$ are the vertically and horizontally polarized components of the emission signal. G is an instrumental correction factor, determined by performing the experiment with a solution of ErIA-labeled bovine serum albumin in 98% glycerol and adjusting G to give a residual anisotropy value of zero, the theoretical value for an isotropically tumbling chromophore. The rotational correlation times Φ_i, amplitudes r_i, and the final anisotropy r_∞ were determined by fitting the anisotropy to a sum of n exponential terms and a constant:

$$r(t) = \sum_{i=1}^{n} r_i(t) \exp(-t/\Phi_i) + r_\infty \quad (3)$$

The data were fitted in the time window from 3 to 500 μs. The fit was optimal for n = 2, with the residual less than 1.5% of the maximum anisotropy. The fitted residual anisotropy r_∞ was within 10% of the calculated average $r(t)$
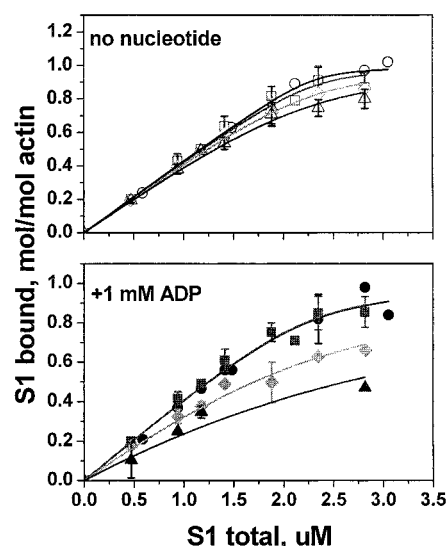

FIGURE 1: Binding of S1 to WT (○) and mutant actins, 4Ac (□), E99A/E100A (◇), and I341A (△), in the absence (top, empty symbols) and the presence (bottom, filled symbols) of 1 mM ADP. Buffer: 1 mM $MgCl_2$ and 10 mM Tris, pH 7.5, 25 °C. Error bars represent standard deviation in two to five independent measurements. Curves show the fit of the data to eq 1.

in the 400−500 μs time range, indicating that the decay reached a plateau level within the analyzed time window.

Reagents. The phosphorescent dye ErIA and fluorescent dye IAEDANS were purchased from Molecular Probes (Eugene, OR) and stored at −20 °C. Protease inhibitors, ATP, phalloidin, and Dowex 1 were obtained form Sigma (St. Louis, MO). All other chemicals were of reagent grade.

RESULTS

Properties of Mutant Actins Used for Spectroscopic Experiments. The functional properties of mutant actins prepared in this study are in agreement with previous reports (*5, 8, 20*). The actin-activated ATPase was increased (V_{max} = 9.3 ± 2.4 s^{-1}, K_m = 11.4 ± 5.9, n = 3) by the 4Ac mutation in comparison with wild-type (WT) yeast actin (V_{max} = 4.8 ± 0.3 s^{-1}, K_m = 17.3 ± 5.6, n = 3) and decreased by mutation I341A (V_{max} = 1.4 s^{-1}, K_m = 58.3). The E99A/E100A mutation resulted in such substantial inhibition of the ATPase that precise determination of V_{max} and K_m was not possible, as described previously (*6, 7, 19*). These functional differences were not affected by labeling with spectroscopic probes ErIA and IAEDANS, as we reported previously (*23*).

The nucleotide removal procedure, described in Materials and Methods, was accompanied by control experiments to ensure that activation of myosin ATPase and binding to S1 (in the presence of ADP) were not affected. Control experiments on actin preparations before and after Dowex treatment showed that the microsecond time scale dynamics (TPA) and appearance of filaments in electron and optical microscopy were not affected.

Binding of S1 to WT and Mutant Actins: Effect of ADP. To determine the effects of S1 binding and ADP on actin structural dynamics, it was necessary to measure S1 binding to actin under conditions of spectroscopic experiments. The binding was determined directly by cosedimentation (Figure 1). Labeling did not have significant effects on binding, so

Table 1: K_d (μM) of S1 for Yeast WT and Mutant Actins[a]

actin	1 mM MgCl$_2$	1 mM MgCl$_2$ and 0.1 M KCl	1 mM MgCl$_2$ and 1 mM ADP	1 mM MgCl$_2$, 1 mM ADP, and 0.1 M KCl
WT	0.02 ± 0.01	0.11 ± 0.03	0.10 ± 0.03	2.18 ± 0.30
4Ac	0.04 ± 0.02	0.09 ± 0.02	0.09 ± 0.02	0.93 ± 0.07
E99A/E100A	0.09 ± 0.01	0.38 ± 0.05	0.55 ± 0.06	5.85 ± 1.07
I341A	0.17 ± 0.03	1.29 ± 0.09	1.47 ± 0.30	75.4 ± 38.59

[a] K_d of S1 for yeast WT and mutant actins obtained by fitting data to eq 1. The data are shown as the mean ± SD obtained from two to five independent measurements.

the results are presented as averages of several measurements on labeled and unlabeled actin. The dissociation constants K_d were obtained by fitting the data to eq 1 (Table 1). In the absence of nucleotide and at low ionic strength (1 mM MgCl$_2$, no KCl), S1 bound to all actins nearly stoichiometrically. Slightly higher K_d values were observed for the E99A/E100A and I341A actins than for the WT and 4Ac actins (Table 1), showing that the inhibitory mutations decreased the affinity of actin for S1, as previously reported (6, 8). Since those previous studies measured the affinities only at higher ionic strength (0.1 M KCl), we repeated our measurements under those conditions and obtained essentially similar results (Table 1). Control experiments with muscle actin gave $K_d = 0.03$ μM, which was also within the range of previously reported values ($K_d = 0.004-0.03$ μM) (27, 28).

We observed that the addition of ADP increased K_d for S1, and the differences between dissociation constants for functionally impaired mutants (E99A/E100A, I341A) and WT or 4Ac became more clear than in the absence of nucleotide (Figure 1, Table 1). This ADP-induced decrease in affinity of S1 for yeast actin was much more pronounced than that previously reported for muscle actin (21, 32−35), especially at higher ionic strength (1 mM ADP + 0.1 M KCl). In the presence of ADP, the affinity of S1 for E99A/E100A was about 3−6 times weaker than for WT actin, and the affinity for I341A actin was several times weaker still (Table 1).

The results obtained in the sedimentation assay were independently confirmed by measuring light scattering of acto-S1 complexes. The ADP-induced decrease in light scattering was much more pronounced for the I341A acto-S1 than for WT acto-S1, and light scattering of the I341A−S1 complex in the presence of 0.1 M KCl and 1 mM ADP became close to that obtained by dissociating the complex in 1 mM ATP. The light scattering measurements were also consistent with weaker binding of S1 to the E99A/E100A than to WT actin, as indicated in the sedimentation assay (Table 1).

The observed inhibitory effect of the E99A/E1000A mutation on strong binding to S1 (Figure 1, Table 1) is similar to the effect of the E93K mutation in *Drosophila* actin (10). This suggests that mutations in the region of weak binding may have allosteric effects on regions of actin crucial for strong interactions. Another possibility is that the regions of weak interactions proposed for skeletal muscle actin may be only partially applicable to yeast actin: the 3D analysis of electron micrographs of negatively stained filaments showed that the amino acid substitutions in yeast actin monomers result in subtle structural changes in F-actin (36).

Effect of Mutations on the Structure and Dynamics of Actin. TPA experiments showed that mutant actins, like WT and muscle actin, are rotationally mobile in the microsecond
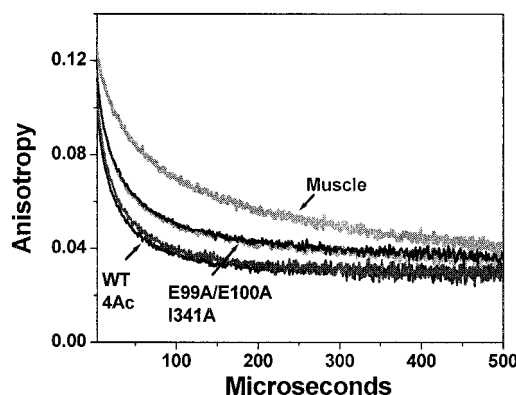

FIGURE 2: TPA of ErIA-labeled yeast WT and mutant actins, compared to TPA of ErIA-labeled muscle actin. Buffer: 1 mM MgCl$_2$ and 10 mM Tris, pH 7.5, 25 °C.

time scale (Figure 2). Yeast actin exhibits greater rotational mobility, in terms of both amplitude (which decreases the final anisotropy r_∞) and rate (decreasing the correlation times Φ_i), as we have shown previously (25), and mutations cause significant effects on these motions (Table 2). The correlation times of actins with the two inhibitory mutations E99A/E100A and I341A were similar to each other but significantly greater (slower) in comparison to WT actin (Table 2), showing that the observed changes in actin's dynamics are correlated with inhibitory functional effects. The slower motions in the functionally impaired mutant actins are consistent with our previous results (16, 23) showing that structural perturbations inhibiting functional interaction with myosin affect the microsecond rotational dynamics of actin.

On the other hand, the stimulating mutation 4Ac, which makes yeast actin more similar to muscle actin at least at the N-terminus, did not have a significant effect on the dynamics. The final anisotropy r_∞ and correlation times of the rotational motions Φ_1 and Φ_2 of the 4Ac mutants remained essentially the same as for WT actin (Figure 2, Table 2).

The inhibitory mutations only slightly increased the phosphorescence lifetimes t of actin-bound ErIA: $t = 93.6 \pm 5.3$ μs for I341A and $t = 90.5 \pm 3.1$ μs for E99A/E100A were less than 20% higher in comparison with $t = 78.2 \pm 1.91$ μs for the WT actin or $t = 81.8 \pm 7.8$ μs for 4Ac, indicating that the exposure of the dye to the solvent was only slightly affected. The maxima of the fluorescence emission spectra were the same (476 ± 1 nm) for all IAEDANS-labeled actins, indicating that the mutation-induced changes in the environment of the C-terminus were not very significant. We concluded that changes detected by TPA reflect changes in actin dynamics rather than changes in the probe environment.

Table 2: Effect of Mutations on the Microsecond Dynamics of Actin Detected by TPA[a]

	no S1			+S1		
actin	Φ_1, μs	Φ_2, μs	r_∞	Φ_1, μs	Φ_2, μs	r_∞
WT	10.6 ± 3.1	59.8 ± 17.9	0.031 ± 0.004	25.6 ± 0.80	275.3 ± 6.81	0.061 ± 0.007
4Ac	8.13 ± 3.10	46.6 ± 13.45	0.036 ± 0.008	22.93 ± 0.67	283 ± 31.7	0.065 ± 0.001
E99A/E100A	15.45 ± 0.21	102.1 ± 4.10	0.033 ± 0.003	23.1 ± 1.50	290 ± 21.82	0.059 ± 0.005
I341A	16.4 ± 0.91	100.32 ± 4.09	0.039 ± 0.002	25.06 ± 3.34	304.4 ± 35.08	0.071 ± 0.004

[a] +S1: 1 mol of S1 added/mol of actin. Buffer: 1 mM $MgCl_2$ and 10 mM Tris, pH 7.5, 25 °C. The data are shown as the mean $\pm$ SD obtained from fitting two to five independent data files to eq 3.
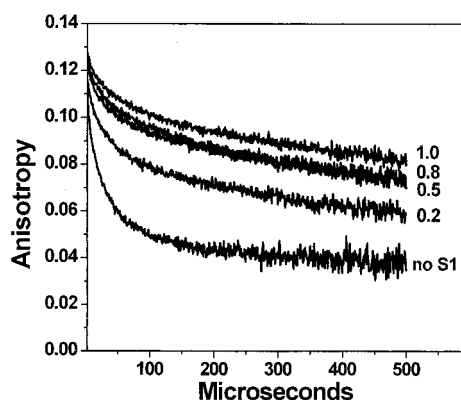

FIGURE 3: Effect of S1 on TPA of ErIA-labeled I341A actin. The molar ratio of S1 added to actin is indicated. Buffer: 1 mM $MgCl_2$ and 10 mM Tris, pH 7.5, 25 °C.
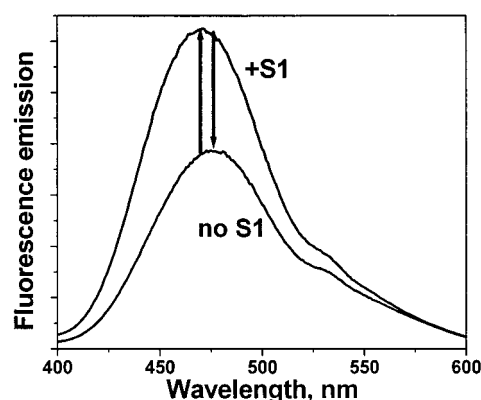

FIGURE 4: Effect of S1 on fluorescence emission spectrum (excitation at 345 nm) of IAEDANS-labeled I341A actin. Arrows show emission maxima in the absence and presence of S1 (molar ratio 1:1). Buffer: 1 mM $MgCl_2$ and 10 mM Tris, pH 7.5, 25 °C.

Effect of S1 on the Dynamics and Structure of WT and Mutant Actins Measured by TPA and Fluorescence. The addition of increasing amounts of S1 to WT and mutant actins in the absence of nucleotide decreased actin's microsecond rotational mobility, as evidenced by decreased angular amplitude (increased the TPA final anisotropy r_∞) and rates (increased the TPA correlation times Φ_i) of ErIA-labeled mutant actins (Figure 3, Table 2), as reported previously for muscle and WT actins (*16*, *23*). We have demonstrated previously that this is due to the restriction of intrafilament motions, not to changes in the overall rigid-body rotations of the actin filament (*15*, *16*). This S1-induced restriction of actin's dynamics was accompanied by a significant change in the local environment of Cys 374, as indicated by a substantial increase in IAEDANS fluorescence intensity, a blue shift of the fluorescence emission maximum from 476 to 471 nm (Figure 4), and a more than 2-fold increase in the phosphorescence lifetime of ErIA to $t = 220.8 \pm 28.8$ μs ($n = 15$).

Since actin mutations had profound effects on S1 binding, the effects of *bound* S1 on the structural dynamics were compared by expressing the observed spectroscopic parameters as a function of bound S1 per actin monomer (Figure 5). The effects of mutations on the correlation times decreased with increasing amounts of bound S1; above 0.5 mol of bound S1/mol of actin both Φ_2 (Figure 5, top) and Φ_1 (data not shown) were unaffected by mutation. The effect of increasing amounts of the bound S1 on fluorescence intensities (Figure 5, bottom) and final anisotropies (data not shown) was the same for all actins. Furthermore, the results obtained in 1 mM $MgCl_2$ and the absence of nucleotide (Figure 5, open symbols) were essentially the same as obtained in the presence of 1 mM ADP, both in TPA and fluorescence experiments (Figure 5, closed symbols), indicating that the structural changes were independent of the ADP-
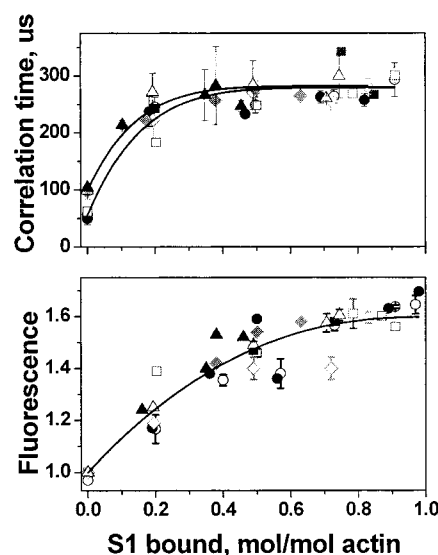
FIGURE 5: Effect of bound S1 on TPA correlation time Φ_2 (top) and fluorescence intensity (bottom) of WT (○) and mutant actins, 4Ac (□), 99A/E100A (◇), and I341A (△), showing fits to the linear lattice model. Buffer: 1 mM $MgCl_2$ and 10 mM Tris, pH 7.5 (open symbols), plus 1 mM ADP (closed symbols). Each point represents the mean $\pm$ SD ($n = 2-5$). Bound S1 was determined as in Figure 1.

induced decrease in affinities. The data were fitted to the "linear lattice" model (*37*), $Y = Y_{max} - (Y_{max} - Y_{actin})(1 - x)^N$, where x is moles of S1 bound per mol of actin, Y_{actin} and Y_{max} are the data values observed at $x = 0$ and 1, respectively, and N is the number of actin monomers affected by one bound S1. $N > 1$ indicates cooperativity, where changes induced in one monomer are propagated along the filament to the neighboring monomers. The changes in Φ_2 showed a high degree of cooperativity for all actins: $N =$

6.3 ± 1.0 for WT and 4Ac, and $N = 7.0 \pm 0.9$ for E99A/E100A and I341A. Similar N's were obtained for Φ_1 ($N = 10 \pm 4$ for WT and 4Ac, and $N = 5.7 \pm 1.2$ for E99A/E110A and I341A; data not shown). Lower cooperativity was observed for the changes in fluorescence ($N = 2.4 \pm 0.2$, Figure 5) and final anisotropy ($N = 2.8 \pm 0.9$), as reported previously for skeletal muscle actin (*16*). These results suggest that S1-induced changes in the local environment of the probe and angular amplitudes of motions are propagated along shorter segments of the filament than changes in the rates of motions. Interestingly, the extent of cooperativity was not affected by mutations, indicating that mutation-induced changes in structural dynamics of actin filaments are less pronounced that changes previously induced by extensive chemical cross-linking and antibody binding (*16*).

Figure 5 shows the effects of bound S1 only at low ionic strength (no added KCl). At higher ionic strength (0.1 M KCl), the results were inconclusive, since binding was weak and there were slow time-dependent changes, probably due to filament aggregation, as previously observed (*16, 38*).

DISCUSSION

Effects of Mutations on Strong Binding to Myosin. The present study confirms the previously reported (*5, 6, 8*) inhibitory effects of specific actin mutations on affinity for myosin, under conditions normally associated with strong actomyosin binding (no nucleotide or ADP bound to myosin). In previous studies on the skeletal muscle actin—myosin system (*21, 35*), the dissociating effect of ADP has been attributed solely to nucleotide-induced changes in the structural state of S1, but the present study provides evidence that the affinity of S1·ADP for actin is also dependent on the structural state of actin, as characterized by structural dynamics of the actin filament. Thus, our data support the proposal (*6, 8*) that mutations in actin affect functional interactions by perturbing equilibria among the major structural states of the actomyosin ATPase cycle.

Effects of Mutations on the Structure and Dynamics of Actin Alone and in the Complex with S1. The present study applied site-specific structural probes of actin under conditions where point mutations affect actin—myosin affinity to test the role of structural dynamics of mutant actin in the absence and presence of bound S1. TPA experiments revealed that mutations decreasing the catalytic efficiency of actin (E99A/E100A and I341A) decreased the rates (increased the correlation times) of microsecond rotational motions (of actin in the absence of S1; Table 2, left side). Thus the present work, consistently with our previous results obtained with modified actin (*16, 23*), supports a correlation between changes in structural dynamics of actin, measured by the probe at Cys 374, and inhibition of functional interactions. The difference between the present and previous results is quantitative: the mutation-induced changes are less pronounced than changes induced by chemical modifications in vitro or by the multiple amino acid substitutions between yeast and muscle actin (*16, 23*). Such quantitative differences in the structural effects of the in vitro and naturally induced functional perturbations are consistent with the differences in their biological impact. Actin is an essential protein for yeast, and therefore, mutation-induced structural and func-

tional changes must be sufficiently mild to support the life of the cell. For example, the known toxicity of muscle actin for yeast cells is probably due to structural differences between the two actins. On the other hand, since in vitro modifications are not limited to those with mild physiological effects, that approach permits the study of larger structural and functional perturbations.

The present experiments with mutant actins allowed us to test the proposal (*16, 23*) that functionally effective modifications and amino acid substitutions affect actin's structural dynamics, as detected by probes at the C-terminus, via allosteric changes in the myosin-binding sites. The crystal structure of actin clearly indicates that the mutated myosin-binding regions are distant from the labeled Cys 374 at the C-terminus. Assuming that distances in yeast actin are similar to distances in muscle actin, Cys 374 is about 26 Å from I341 and 22−23 Å from E99 and E100, and these distances are greater than the sizes (10−15 Å) of our optical probes. Thus, the Cys 374-bound probes are too distant from the sites of mutations to be affected directly. The lack of structural effects due to mutation 4Ac is puzzling, since this mutation seems to increase the catalytic efficiency of actin-activated ATPase without a detectable effect on actin's structure. A possible explanation is that the transmission of structural changes to Cys 374 (about 24 Å) is impaired by the high degree of disorder within the extreme N-terminus (where the 4Ac is located), as indicated in electron microscope reconstructions (*39*). However, this disorder did not prevent a decrease in the rates of the microsecond motions measured at Cys 374 upon binding a specific antibody to the first seven residues (*16*). Since that antibody inhibits activation of myosin ATPase (*40*), while the 4Ac mutation stimulates the ATPase, our data suggest that *inhibitory and stimulatory perturbations of actin's structure have opposite effects on actin's dynamics*. On the other hand, the molecular mechanism of the effects of the 4Ac mutation may be related to the mechanism of increasing K_m, which is not the equivalent of binding affinity but rather reflects the equilibrium among the structural states of the rate-determining transient complexes at the end of the actomyosin ATPase cycle (*41*). This possibility has been previously proposed (*6*), but it has not yet been tested.

The Structural Changes Observed by Spectroscopy in the Absence of S1 Were Eliminated by S1 Binding, in both the Absence and Presence of ADP. The TPA and fluorescence were independent of mutation once saturating amounts of S1 were bound (Table 2, right side; Figure 5). This conclusion is consistent with our previous studies on the effects of structural perturbations of actin, where the TPA decays (correlation times and anisotropies) of strongly bound acto-S1 complexes were independent of structural and functional perturbations of actin and were similar to that observed for unmodified muscle acto-S1 (*16, 23*). In those studies the main effects of perturbations were changes in the structural dynamics of actin alone and in decreasing the extent of the S1-induced changes, *without changing the end point observed at saturating S1*, as observed in the present study (Table 2, Figure 5).

In the absence of a mutation-induced change in the structural dynamics of the strongly bound complex (right side of Table 2) despite a substantial change in the absence of S1 (left side of Table 2), we suggest that the functional

perturbations caused by mutations are due to a shift in equilibrium between dynamic structural states of actin. The results of binding assays and spectroscopic measurements can be explained if we assume that actomyosin affinity depends not only on the state of the myosin−nucleotide complex (weak vs strong) but also on the state of actin. The hypothesis is that actin has two (or more) structural states that bind myosin heads with different affinities or that have differential affinities for the weakly and strongly bound complexes of the myosin−nucleotide complex. The proposal that actin filaments can assume multiple structural states has received support recently from electron microscopy (*42*), and our previous work has shown that structural changes detected by electron microscopy correlate with changes in dynamics detected by TPA (*43*). If structural effects of mutations detected by our TPA measurements represent a shift of equilibrium toward structural states characterized by lower affinities for myosin, this would decrease the apparent affinity of strong binding (Figure 1) without affecting the structure of the strong complex (Figure 5).

On the other hand, a direct effect of mutations on the structure of the strongly bound actomyosin complex cannot yet be eliminated. There is still a possibility that results obtained by monitoring probes located at only one site and detecting allosteric effects still cannot provide all information concerning the relationship between the structure of actin in the strongly bound complex and the functional state of actomyosin. Furthermore, the present spectroscopic measurements were limited to the strong-binding states at the final stage of the actomyosin ATPase cycle, but the effect of myosin on actin at the preceding weak-binding states (M·ATP, M·ADP·P$_i$) of the cycle remains unknown. There have been efforts to detect the effect of myosin on actin during these weak interactions, but the reported effects are controversial. Experiments that measure global dynamics of actin, e.g., microscopy and TPA, indicated that myosin perturbs actin structure in weakly bound states (*12*, *44*). Saturation transfer EPR studies of the microsecond dynamics of actin indicate equal effects of myosin on actin during weak and strong interactions (*47*). On the other hand, the fluorescence of actin labeled with pyrene iodoacetamide at Cys 374 indicates that myosin perturbs the local environment of this probe only in the strongly bound, but not in the weakly bound, states (*45*), while experiments with the same pyrene attached to a different site, Cys1 in mutant yeast actin, indicated that the effect of myosin is more pronounced in the weakly bound than in the strongly bound state (*46*). Thus, understanding of the role of myosin-induced changes in actin structure in the mechanism of functional interactions with myosin requires more studies, including structural transitions in weakly bound states.

REFERENCES

1. Holmes, K., Popp, D., Gebhard, W., and Kabsch, W. (1990) *Nature 347*, 44−49.

2. Rayment, I., Rypniewski, W. R., Schmidt-Base, K., Smith, R., Tomchick, D. R., Benning, M. M., Winkelmann, D. A., Wesenberg, G., and Holden, H. M. (1993) *Science 261*, 50−58.

3. Rayment, I., Holden, H. M., Whittaker, M., Yohn, C. B., Lorenz, M., Holmes, K. C., and Milligan, R. A. (1993) *Science 261*, 58−64.

4. Mendelson, R., and Morris, E. P. (1997) *Proc. Natl. Acad. Sci. U.S.A. 94*, 8533−8538.

5. Miller, C. J., and Reisler, E. (1995) *Biochemistry 34*, 2694−2700.

6. Miller, C. J., Wong, W. W., Bobkova, E., Rubenstein, P., and Reisler, E. (1996) *Biochemistry 35*, 16557−16565.

7. Wong, W. W., Doyle, T. C., and Reisler, E. (1999) *Biochemistry 38*, 1365−1370.

8. Miller, C. J., Doyle, T. C., Bobkova, E., Botstein, D., and Reisler, E. (1996) *Biochemistry 35*, 3670−3676.

9. Johara, M., Toyoshima, Y. Y., Ishijima, A., Kojima, H., Yanagida, T., and Sutoh, K. (1993) *Proc. Natl. Acad. Sci. U.S.A. 90*, 2127−2131.

10. Razzaq, A., Schmitz, S., Veigelt, C., Molloy, J. E., Geeves, M., and Sparrow, J. C. (1999) *J. Biol. Chem. 274*, 28321−28328.

11. Takebayashi, T., Morita, Y., and Oosawa, F. (1997) *Biochim. Biophys. Acta 492*, 357−363.

12. Yanagida, T., Nakase, M., Nishiyama, K., and Oosawa, F. (1984) *Nature 307*, 58−60.

13. Tsuda, Y., Yasutake, H., Ishijima, A., and Yanagida, T. (1996) *Proc. Natl. Acad. Sci. U.S.A. 93*, 12937−12942.

14. Sase, I., Miyata, H., Ishiwata, S., and Kinoshita, K. (1997) *Proc. Natl. Acad. Sci. U.S.A. 94*, 5646−5650.

15. Prochniewicz, E., Zhang, Q., Howard, E., and Thomas, D. D. (1996) *J. Mol. Biol. 255*, 446−457.

16. Prochniewicz, E., and Thomas, D. D. (1997) *Biochemistry 36*, 12845−12853.

17. Miki, M., M., Wahl, P., and Auchet, J. C. (1982) *Biochemistry 21*, 3661−3665.

18. Prochniewicz, E., and Yanagida, T. (1990) *J. Mol. Biol. 216*, 761−772.

19. Kim, E., Bobkova, E., Miller, C. J., Orlova, A., Hegyi, G., Egelman, E., Muhlrad, A., and Reisler, E. (1998) *Biochemistry 37*, 17801−17809.

20. Cook, R. K., Root, D., Miller, C. Reisler, E., and Rubenstein, P. (1993) *J. Biol. Chem. 268*, 2410−2415.

21. Geeves, M. A. (1989) *Biochemistry 28*, 5864−5871.

22. Weeds, A. G., and Pope, B. (1977) *J. Mol. Biol. 111*, 129−157.

23. Prochniewicz, E., and Thomas, D. D. (1999) *Biochemistry 38*, 14860−14867.

24. Frieden, C., Lieberman, D., and Gilbert, H. R. (1980) *J. Biol. Chem. 255*, 8991−8993.

25. dos Remedios, C. G., Miki, M., and Barden, J. (1987) *J. Muscle Res. Cell Motil. 8*, 97−117.

26. Bradford, M. M. (1976) *Anal. Biochem. 72*, 248−254.

27. Miller, C. J., Cheung, P., White, P., and Reisler, E. (1995) *Biophys. J. 68*, 50s−54s.

28. Lanzetta, P. A., Alvarez, L. J., Reinach, P. S., and Candia, A. (1979) *Anal. Biochem. 100*, 95−97.

29. Eads, T. M., Thomas, D. D., and Austin, R. H. (1984) *J. Mol. Biol. 179*, 55−81.

30. Marston, S., and Weber, A.-M. (1975) *Biochemistry 14*, 3868−3873.

31. Katoh, T., and Morita, F. (1996) *J. Biochem. 120*, 189−192.

32. Greene, L. E., and Eisenberg, E. (1980) *J. Biol. Chem. 255*, 543−548.

33. Greene, L. E. (1981) *Biochemistry 20*, 2120−2126.

34. Highsmith, S. (1990) *Biochemistry 29*, 10690−10694.

35. Trybus, K. M., and Taylor, E. (1982) *Biochemistry 21*, 1284−1294.

36. Orlova, A., Chen, X., Rubenstein, P. A., and Egelman, E. H. (1997) *J. Mol. Biol. 271*, 235−243.

37. McGhee, J. D., and von Hippel, P. H. (1974) *J. Mol. Biol. 86*, 469−489.

38. Ando, T., and Scales, D. (1985) *J. Biol. Chem. 260*, 2321−2327.

39. Orlova, A., Xiong, Y., and Egelman, E. H. (1994) *Biophys. J. 66*, 276−285.

40. DasGupta, G., and Reisler, E. (1992) *Biochemistry 31*, 1836−1841.

41. Lymn, R. W., and Taylor, E. W. (1971) *Biochemistry 10*, 4617−4623.

42. Galkin, V. E., Orlova, A., Lukoyanova, N. A., and Egelman, E. H. (2001) *Biophys. J.*, 96A.

43. Orlova, A., Prochniewicz, E., and Egelman, E. H. (1995) *J. Mol. Biol. 245*, 598−607.

44. Ng, C. M., and Ludescher, R. D. (1994) *Biochemistry 33*, 9098−9104.

45. Geeves, M. A., Jeffries, T. E., and Millar, N. C. (1986) *Biochemistry 25*, 8454−8458.

46. Hansen, J. E., Marner, J., Pavlov, D., Rubenstein, P. A., and Reisler, E. (2000) *Biochemistry 39*, 1792−1799.

47. Ostap, E. M., and Thomas, D. D. (1991) *Biophys. J. 59*, 1235−1241.